

ACOUSTIC PROPAGATION OVER THE CONTINENTAL SLOPE AND DEEP BASIN OFF EASTERN AUSTRALIA

Robin Robertson¹ and Paul Hartlipp¹

¹School of Physical, Environmental, and Mathematical Sciences
UNSW Canberra, Canberra, ACT 2610, Australia
Email: r.robertson@adfa.edu.au

Abstract

Sound propagation in Australian waters is of keen interest to the Royal Australian Navy (RAN) and the Maritime Division of the Royal Australian Air Force (RAAF) as it affects sonar performance in one of their prime operating regions. Off eastern Australia, temperature fields are affected by the East Australian Current (EAC), eddies generated by the EAC, and internal tides. The ocean's temperature structure off eastern Australia can be divided into three basic regimes: the strong southward EAC region (24°-28°S), the EAC separation region (28°-32°S), and the 'river' of eddies region (32°-38°S) south of the separation zone. Although the internal tides in this region are small, they modify the sound speed profile, with the potential to affect acoustic propagation on time scales of the daily and twice daily tidal cycles and the 15-day spring-neap tidal cycle.

A primitive-equation model (Regional Ocean Modelling System (ROMS)) with tidal forcing provided temperature and salinity fields, from which horizontally and vertically dependent sound speed fields for the waters off eastern Australia were generated and saved at hourly intervals for 60 days. Using these sound speed fields and the Bellhop acoustic ray tracing software, the effects of the EAC, eddies and internal tides on sonar propagation were investigated. Both ray paths and Transmission Loss were analysed for dependencies on both latitude and the tidal cycles. Acoustic rays propagation and Transmission Loss at 50 Hz were determined for sound speed fields at 100 different time snapshots, each separated by at least 1 hour for 25 latitude cuts (24°-36°S at 0.5° intervals), for 6 different source depths (2, 50, 100, 200, 300, and 500 m), yielding a total of 15,000 cases.

The two most significant factors in ray propagation and Transmission Loss were latitude and source depth. North of 29°S, there was more Transmission Loss in the first 50 km than south of 29°S. Observation of the rays indicated sound channels formed within two primary depth bands, both centred around 1400 m depth; one 1000 m wide from 900 to 1900 m and a wider channel 2000 m from 400 to 2400 m. More rays propagated within the sound channels with deeper source depths, particularly the narrower (900-1900 m) sound channel. A large eddy was found to disrupt the beam patterns and increase Transmission Loss and an offshore seamount was found to terminate the sound channels that formed at that latitude and also increase Transmission Loss. The sound speed fluctuated with the semidiurnal and diurnal tidal cycles; however, tidal impacts on the acoustic propagation were overwhelmed by that of eddies and topography.

1. Introduction

The primary feature in the waters off eastern Australia is the East Australian Current (EAC). The EAC dominates the circulation in the region, bringing warm water south. Between 28°S and 32°S the EAC

separates from the coast and flows out into the Tasman Sea (Figure 1). South of this separation zone, a ‘river’ of eddies is formed along the shelf break consisting of eddies that have split off of the EAC. This is often called the EAC Extension. Consequently, the waters off eastern Australia can be broken into three regions, 1) a northern region (24°-28°S) with a strong EAC over the continental slope, 2) the EAC separation zone (28°-32°S), and 3) the “river” of eddies region or EAC extension, south of the separation zone (32°-38°S). Eddies also form throughout the path of the EAC and are generated by interactions of the EAC with topography and/or Rossby waves after the EAC separates from the coast.

The EAC and eddies change the structure of the temperature and salinity fields, as can be seen in the potential temperatures of Figure 2a. The strongly slanting isotherms over the continental slope are consistent with the strong geostrophic flow of the EAC (Figure 2). A strong eddy along the transect at 26°S induces a sharp rise in the isotherms at ~105 km along the transect (Figure 2a). Additionally, internal tides and waves generated through interactions of the tides with topography are superimposed on these temperature fields and cause undulations in the isotherms on the order of 50 m in the thermocline around 500 m depth and of 100-200 m deeper in the ocean where the density stratification is weaker (Figure 2). These features alter the temperature structure and consequently the sound speed fields. Furthermore, the temperature fields vary in time due to both the daily and spring-neap tidal cycles, resulting in fluctuations in the temperature, salinity, and sound speed fields.

Propagation of acoustic rays in the ocean depends on temperature, salinity, and density [1]. While pressure is primarily controlled by depth, temperature and salinity vary both spatially and temporally. The effects of eddies and the surface mixed layer were investigated by Jones [2] and

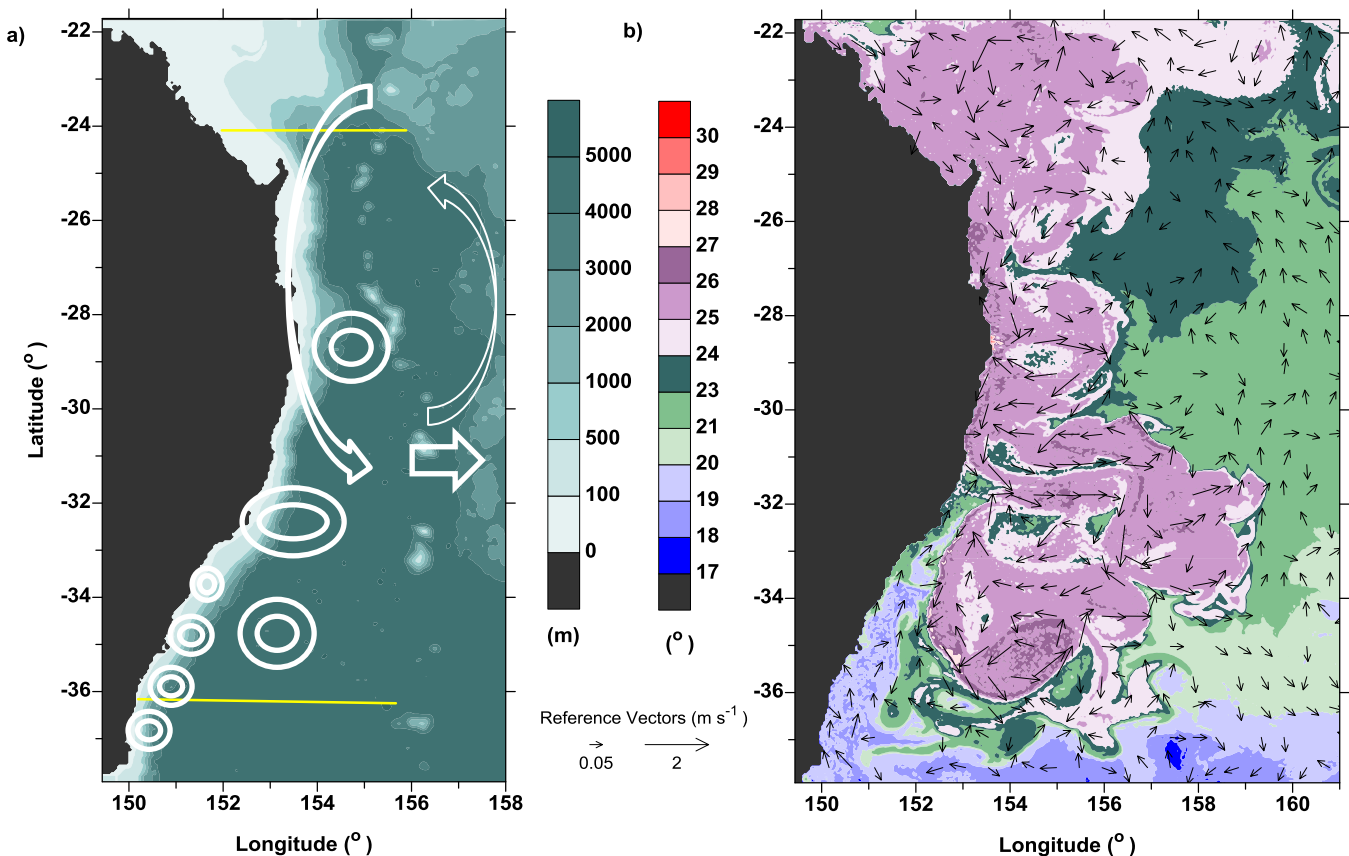


Figure 1. a) The region used for investigation of acoustic propagation. Transects from the continental shelf edge to 250 km offshore at latitudes from 24°S to 36°S at 0.5° intervals were used to investigate acoustic wave propagation (latitude limits of investigation are indicated by yellow lines). The background is the bathymetry off the East coast of Australia. The wide white arrows indicate the general path of the EAC, with the thin arrow representing the recirculation cell, and the white circles represent areas where eddies are present or often present. The entire domain of the simulation is not shown. b) Surface temperatures (colors) at 30 days are shown with vectors representing the surface flow. Several large eddies are present in the domain.

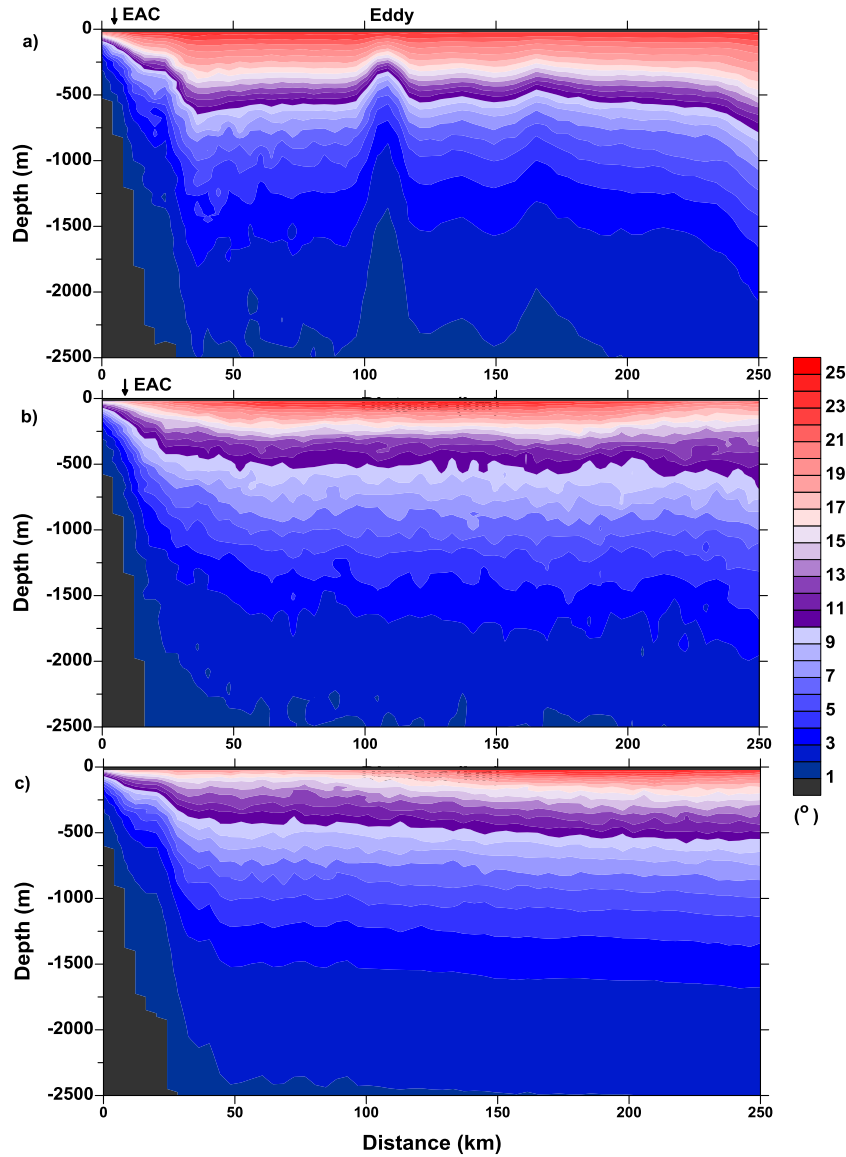


Figure 2. Transects of the temperature with depth for the upper 2500 m at hour 1 during spring tide at a) 26°S, b) 30°S, and c) 36°S

Clements and Robertson [3], respectfully. Using BLUElink model results for the temperature fields, Jones found that eddies induce a highly variable sound speed field, which affected surface duct transmission [2]. Clements and Robertson found that eddies on the continental shelf caused acoustic rays to become trapped in the lower water column beneath the thermocline [3]. Additionally, the “episodic nature of packets of internal waves gives intermittency to some acoustic effects” and affects acoustic propagation [4].

Using temperature and salinity fields for Ombai Strait from a tidal model for the Indonesian seas, Cooper [5] found that a sound channel around 600 m formed and disappeared with the daily, twice-daily, and spring-neap tidal cycles. The number of rays trapped within the sound channel fluctuated with the tides. The limits of the upper and lower limiting rays also fluctuated with the tidal cycles. So in Ombai Strait, there was a strong tidal dependence of the acoustic propagation. Since huge internal tides 50-100 m in height occurred near the permanent pycnocline in this simulation, this was not unexpected. We wanted to investigate the effect of eddies and internal tides on acoustic propagation and Transmission Loss throughout the water column off eastern Australia, while noting the internal tides were much smaller off Australia.

Previously the effects of internal waves on acoustic propagation over the continental shelf off eastern Australia were investigated by tracing acoustic rays over transects at four different latitudes with five different source depths (2 m, 20 m, 50 m, 200 m, and 500m) [3], using temperature fields

from a tidal simulation (Figure 1) [6]. However, Transmission Loss was ignored. Here, we expand this study to deeper waters looking at transects across the continental slope into the deep basin, including Transmission Loss. Again temperature fields were taken from a tidal simulation [6] using 25 transects ranging from 36°S to 24°S at 0.5° intervals (Figure 1) for 6 source depths (2m, 50m, 100 m, 200m, 300m, and 500m.)

2. Ray Tracing

The acoustic rays were traced using the 2-D BELLHOP [7,8] with a 50 Hz frequency source. This program traces acoustic rays through a 2-D sound speed field, which varies both horizontally and vertically. At the source depth, 50 rays with originating angles ranging from -60° to 60° were started for source depths below 2 m. For the 2 m source depth, the angles ranged from -60° to 0°. In our use here, all rays were traced and included in the analysis without regard to receiver depth. To get Transmission Loss, BELLHOP was repeated in the Transmission Loss mode with 500 rays. The horizontal source location was at the continental shelf break when the water depth reached 600 m in all cases.

3. Sound Speed Fields

To provide sound speeds for the waters off eastern Australia, potential temperature and salinity fields during the tidal cycles were determined using temperature and salinity data from a simulation of the region [6]. The hydrodynamic, primitive-equation model used was the Regional Ocean Modelling System (ROMS). ROMS was run for 60 days at a 4 km resolution with realistic, climatological hydrography and tidal forcing. Incoming solar radiation was not included in the simulation, as a result surface ducts are absent. The model and simulation are described more fully in Hartlipp and Robertson [9].

Although there was no local or regional wind forcing, the realistic temperatures and salinity fields set up horizontal pressure gradients, which generated geostrophic currents. A strong, southward current with velocities of 1.5-2 m s⁻¹ and transports of 40-60 Sv was present over the continental slope in the simulations. This current split from the coast ~30-32°S and basically had the characteristics of the EAC (Figure 1b). This current spun off eddies both as it meanders and as it split from the coast, (Figure 1). Offshore, a recirculation cell formed (indicated by the thin northward white arrow in Figure 1a and northward velocities in Figure 1b). It should be noted that the temperatures and velocities in Figure 1 are a snapshot in time at 30 days and both the temperatures and velocities vary in time, although the strong EAC current is robust and present from the beginning of the simulation. The simulation was initiated using a 2-day average of the final temperature, salinity, surface elevation, and velocities fields from a spin-up simulation, which started with realistic initial conditions and was run without tides until the kinetic energy had stabilized. Additionally, below 1000 m, there was a northward current, which had the characteristics of the observed East Australian Undercurrent (EAU) when compared to an 18-month time series from a transect of five Integrated Marine Observing System (IMOS) moorings off 27°S (not shown). Although the EAC and eddies were recreated in this simulation, the circulation in shallow waters was not as well reproduced, due to the highly variable temperature fields there and insufficient initial conditions in that area. The simulations, including comparisons to observations, are detailed in Hartlipp and Robertson [9].

Transects of these hydrographic fields across the continental shelf and slope into the deep basin were used to calculate sound speed profiles at 4 km horizontal intervals. The UNSESCO algorithms for pressure and sound speed were used to convert depth to pressure and calculate the sound speed from the potential temperature, salinity and pressure fields [10]. Since temperature varies with latitude, sound speed fields were investigated along transects across the continental shelf into the deep basin at 25 different latitudes ranging from 24°-36°S, at 0.5° intervals.

Sound speed fields were generated at hourly intervals for each of the 25 latitude transects. Two 50 hour periods, one each for spring, hours 880-929, and neap, hours 1051-1100, tide were selected for this study and are shown in the elevation time series in Figure 3a for 3 different latitudes. Transects of

the sound speed at 26°S (red), 30°S (black), and 36°S (blue) are shown at 3 different depths in Figure 3b-d. In the bottom layer, the sound speed is relatively constant with time; however, at the surface and mid-way down the water column, the sound speed changes with time, showing both trends and fluctuations. The temporal fluctuations indicate the influence of the tidal cycle, particularly in the northern two transects. There is also evidence of other events impacting the sound speeds, such as the presence of eddies.

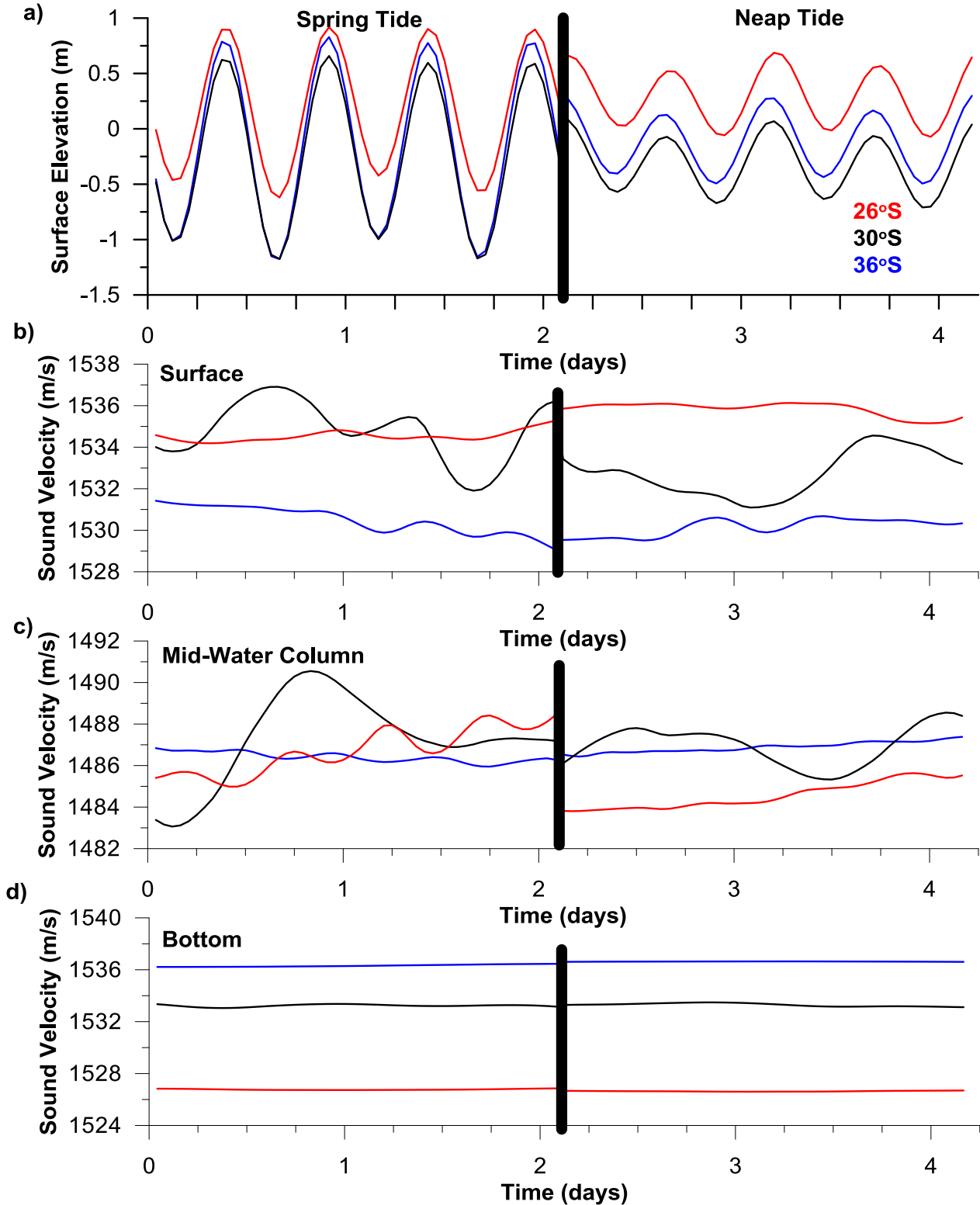


Figure 3. a) Time series of the elevation at a point over the continental slope break at 26°S (red), 30°S (black), and 36°S (blue), from the simulation. Time series of the sound speed at b) the surface, c) halfway through the water column, and c) the bottom at these same points. The thick bar splits the time from the spring time from the time of the neap tide. The spring and neap tides are not contiguous.

4. Sensitivity of the Acoustic Propagation Rays

To evaluate the dependencies both on latitude and the tidal cycles, acoustic ray propagation and Transmission Loss were determined at 100 snapshots for each of the 25 latitude cuts, for 6 different source depths. This yielded 2,500 cases for each of the source depths or 15,000 cases in total. Two of these cases are shown in Figure 4. Both cases in Figure 4 are at the same latitude and time and differ only in source depth. Analysis routines were used to automatically evaluate the characteristics of the ray paths from the large number of cases. The criteria evaluated were the limiting rays, formation of sound channels, and the depth range of the paths. Inspection of the ray paths in Figure 4 showed a high concentration of rays bouncing from close to the surface to 3000-4600 m (black lines) or within the water column, but having touched the bottom at some point (blue lines).

4.1 Ray limits

Neglecting the first 25 km, all rays came within 1400 m of the surface, with most coming within 100 m (Figure 5a and c). Nearly all rays also reached below 2000 m with a majority of them reaching 3000 m (Figure 5b and d). There are some slight variations in the upper limits with the daily tidal cycles, but no appreciable difference in their depths with the spring-neap cycle (Figure 5a and b). Rays reached both higher and deeper in the water column between $27^{\circ}30'$ and $28^{\circ}30'$ S and to a lesser extent near $31^{\circ}S$.

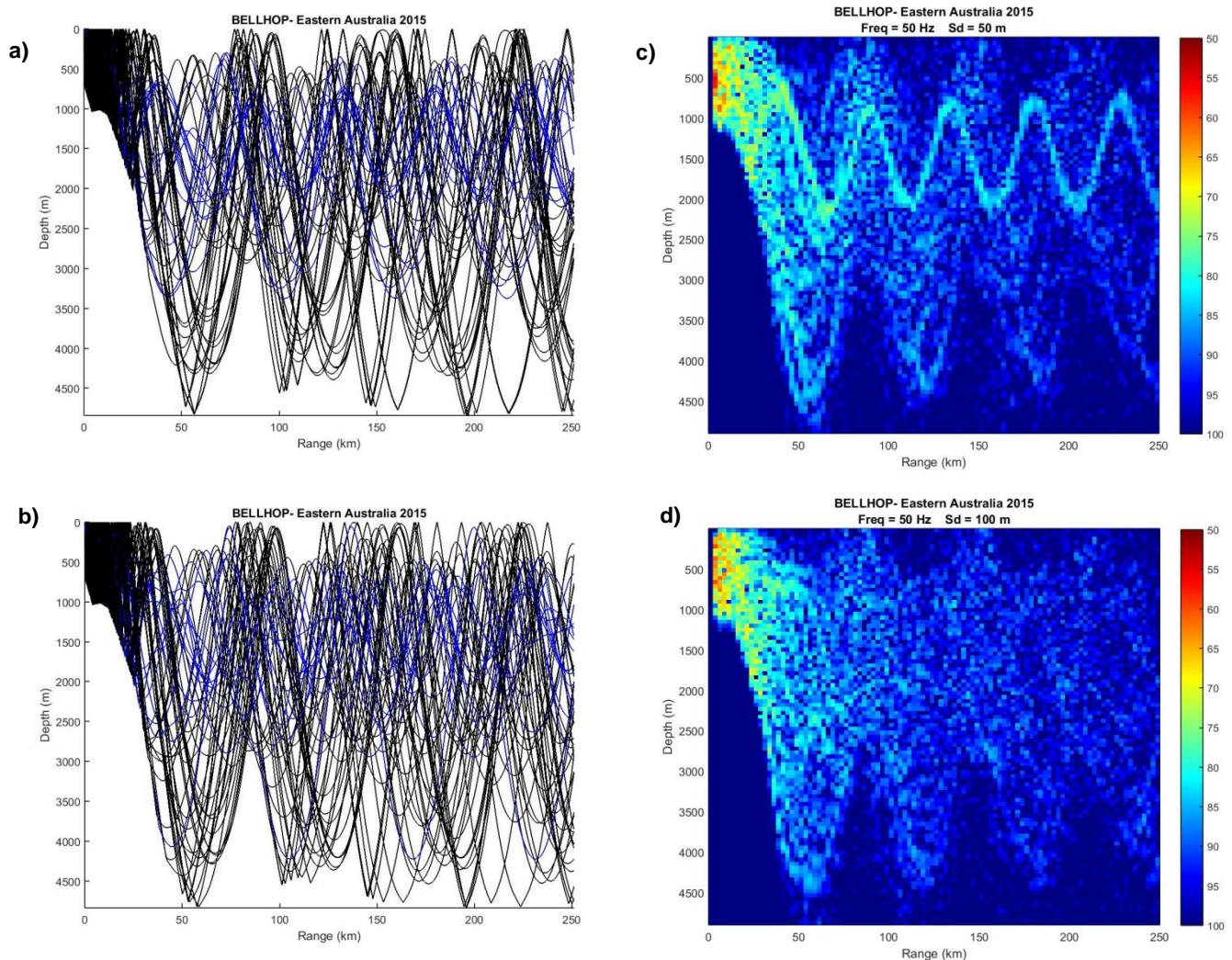


Figure 4. Ray paths for a transect at $30^{\circ}S$ for source depths of a) 50 m and b) 100 m at hour 1052 during neap tide. Transmission Loss at 50 Hz for source depths of c) 50 m and d) 100 m for the same hour. In a) and b), the blue colour indicates a ray that has not touched the surface. In both a) and b), some rays fluctuate around the sound speed minimum, which is ~ 1400 m depth.

4.2 Depth ranges

Like the upper and lower limits, most of the rays, > 50% had depth ranges of ~3000 m or more (Figure 6). Like with the limits in section 4.1, the first 25 km of were ignored. Again, although there were fluctuations with the daily tidal cycles, there was no clear pattern or differences with the spring-neap cycles (Figure 6a). There was a clear increase in the depth range of the rays between 27°30' S and 28°30' S and to a lesser extent near 31°S.

4.3 Sound channels

Acoustic rays bend due to differences in sound speed and bend toward the lower sound speed. If a sound speed minimum occurs at depth, acoustic rays will bend, fluctuating around the sound speed minimum. Sound channels form around such a sound speed minimum, when acoustic rays do not bounce between the surface and the bottom, but propagate within a narrower depth range (Figure 7). Commonly a sound channel exists centred around a depth of 1000-1200 m at low to mid-latitudes. Shallower sound channels can occur when the sound speed minimum occurs in the mid-water column. Although shallow sound channels were found in an earlier study over the continental shelf [6], shallow sound channels were not found in this study over the continental slope and deep basin.

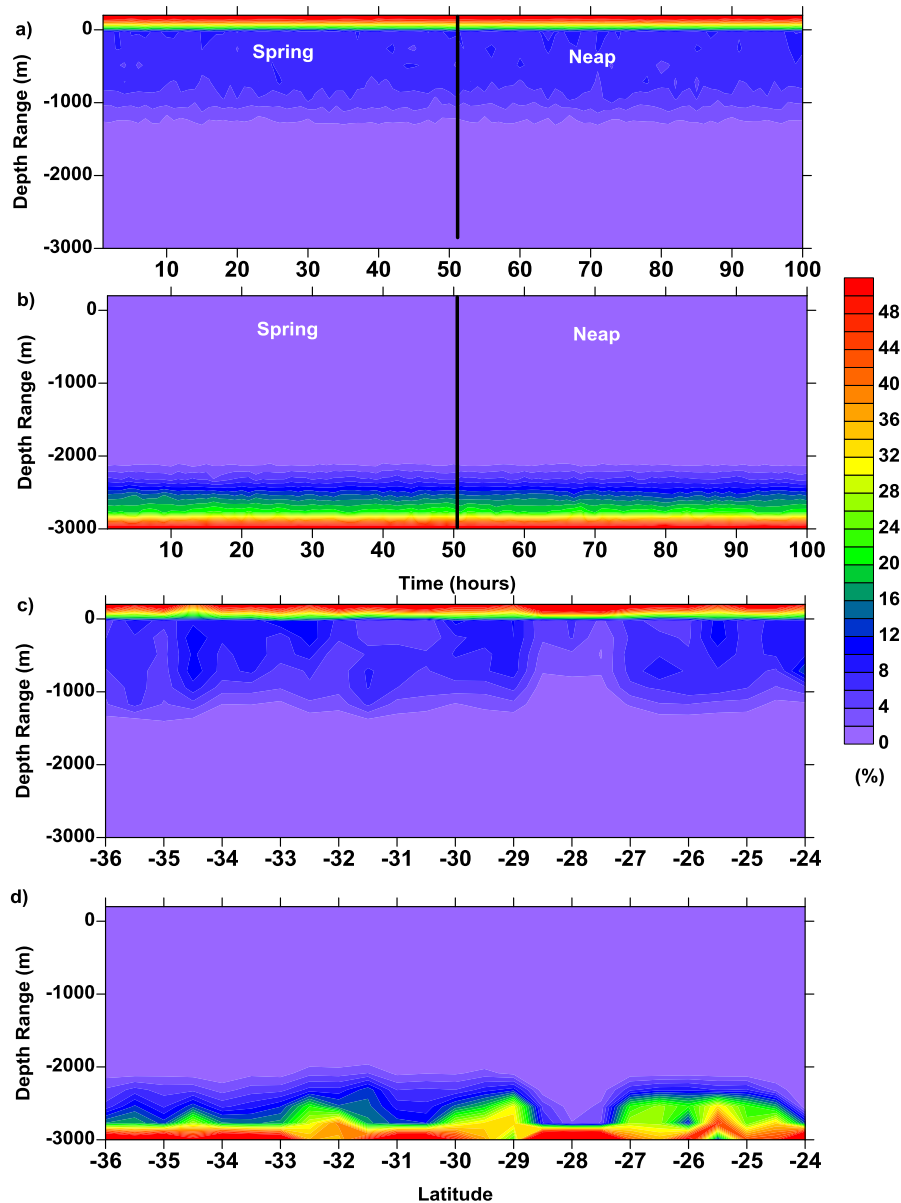


Figure 5. The distribution of the a) upper and b) lower limits of the rays in percentage of rays with time and the distribution of the c) upper and d) lower limits with latitude for all rays with a source depth of 100 m

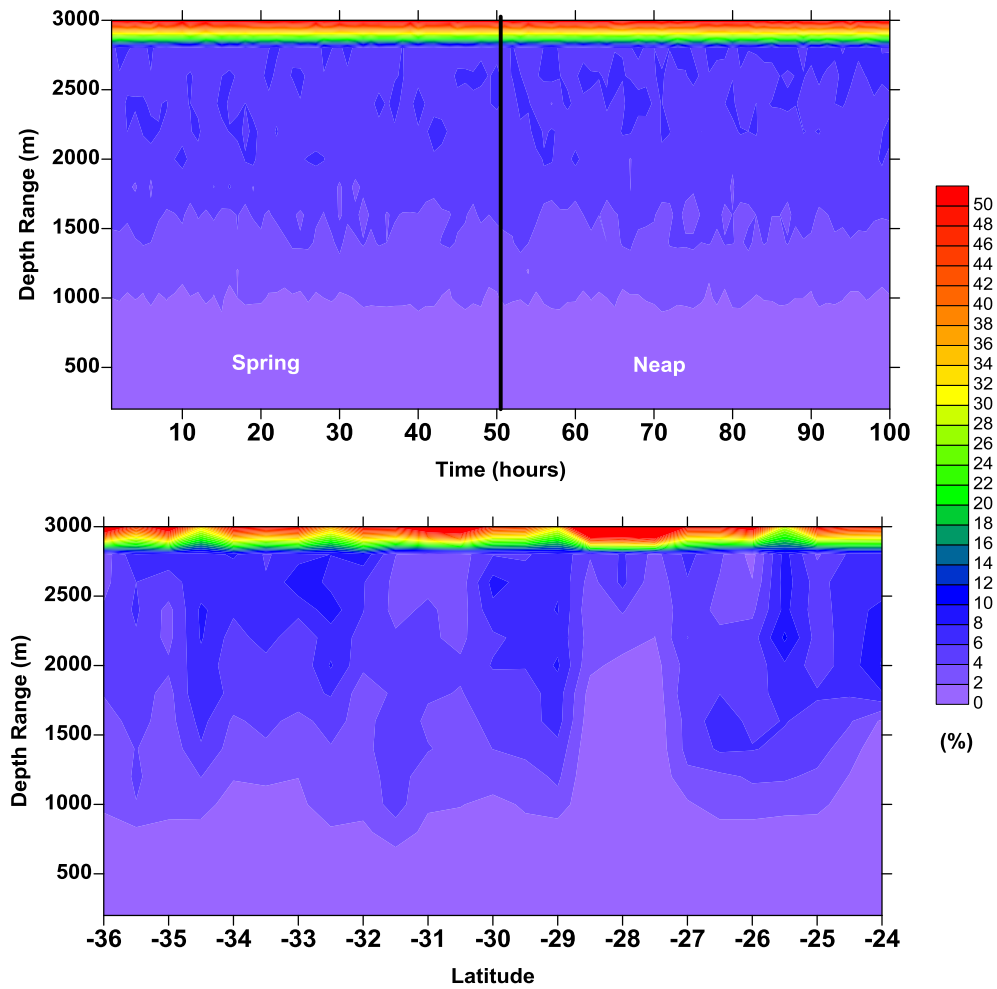


Figure 6. The distribution of the depth ranges for the rays a) with time and b) with latitude for a source depth of 100 m. The first 25 km of the ray was not included

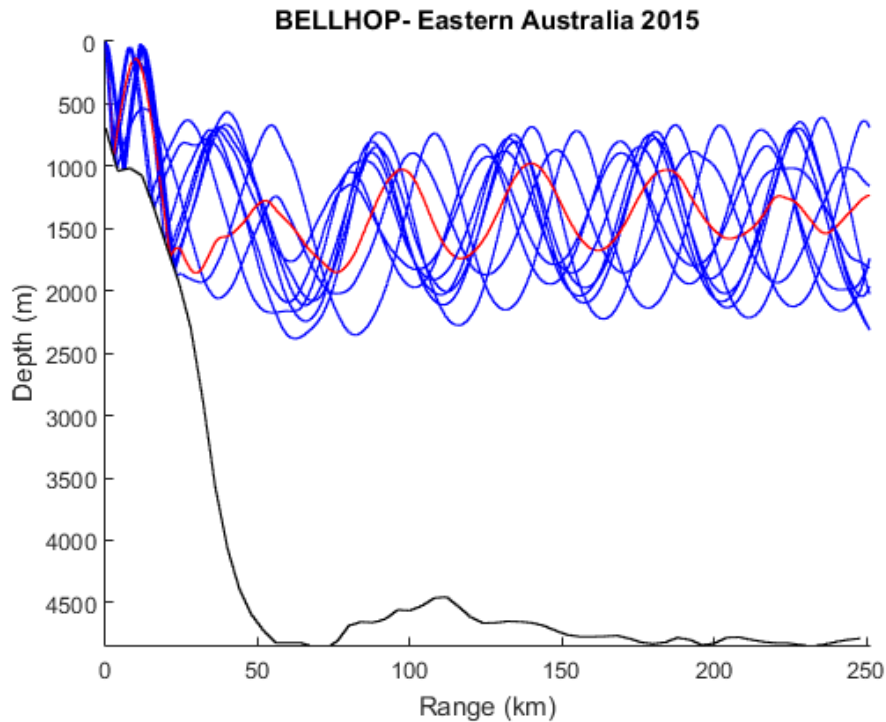


Figure 7. Example of rays trapped in the two sound channels around 1400 m. The red rays are trapped in the narrower channel and the blue in the deep channel. Rays are from the transect at 30°S at hour 1052 for a source depth of 50 m, corresponding to the upper panels in Figure 4

In this study, deep sound channels formed in two primary ranges, both centred on ~ 1400 m; one with a width of 1000 m or less, ranging from ~ 900 m to ~ 1900 m and the other with a width of ~ 2000 m ranging from ~ 400 m to ~ 2400 m (Figure 7). We note that this depth range is a bit deeper than typically in the ocean, 1400 m compared to 1000-1200 m. Like in Figure 7, the sound channels for each case do not always occupy the entire range. The two ranges represent narrower and wider sound channels. As expected, there were more rays in the wider sound channel. The narrower sound channel only occasionally had 1-2 rays in it (Figure 7a). Also there were larger numbers of rays in the sound channels with deeper source depths and fewer with shallower source depths. There was no noticeable dependence on the spring-neap tidal cycle, although daily fluctuations occurred (Figure 8a). For the wider sound channel from 400-2400 m, there was a strong latitude dependence with no rays in it at $\sim 28^\circ\text{S}$ and many rays in the sound channel for bands at $31^\circ 30'$ and $34^\circ 30'$ S (Figure 8b).

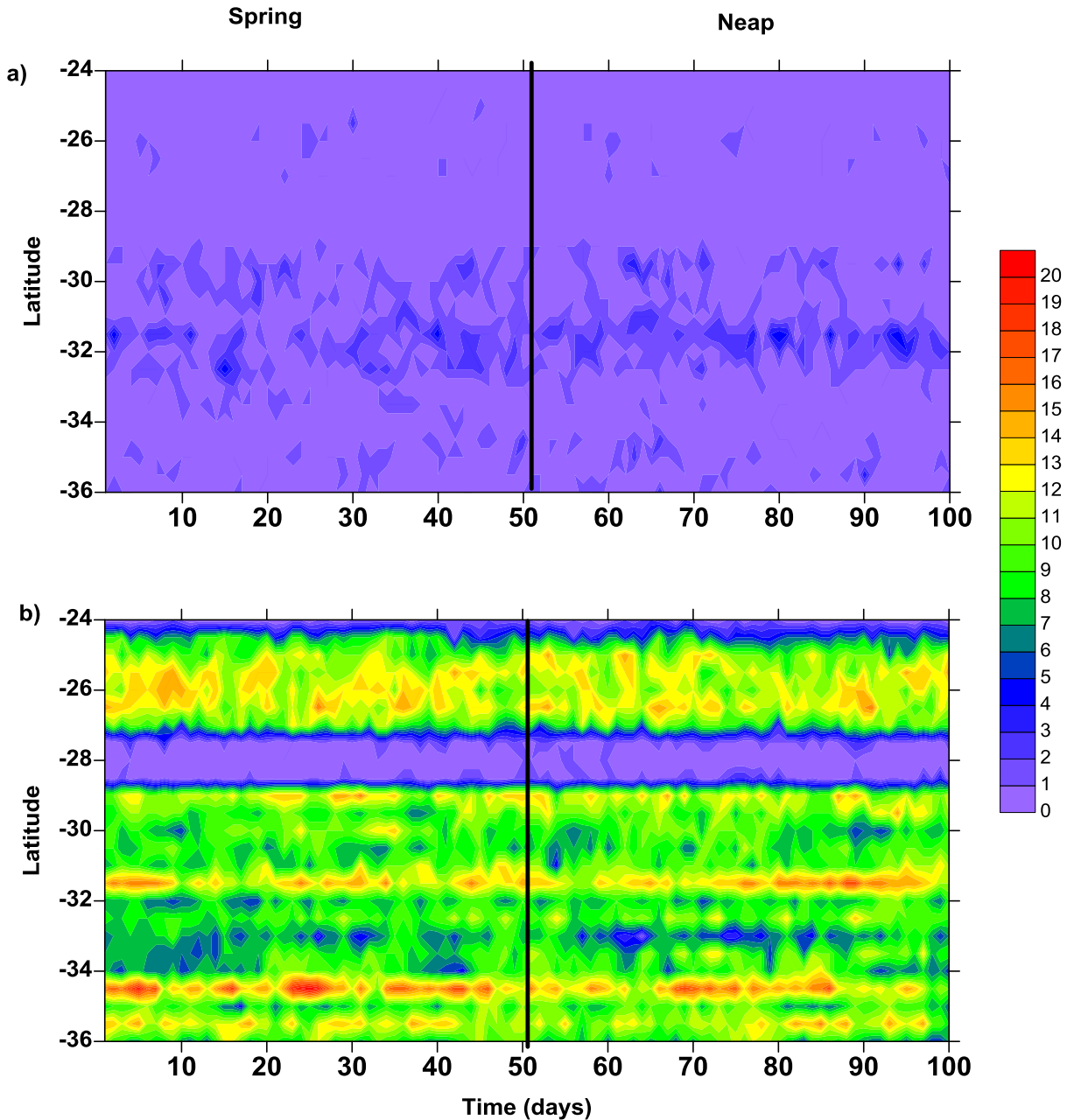


Figure 8. The number of rays within the deep sound channel centred ~ 1400 m with widths of a) 1000 m and b) 2000 m per latitude and time for a source depth at 100 m.

4.4 Sensitivity of transmission loss

To investigate Transmission Loss, the signal strength loss in dB was integrated over the water column and the distance from the source for different times and latitudes (Figure 9a). Transmission Loss was

also integrated over the water column at each distance over both time (Figure 9b) and latitude (Figure 9c). Higher Transmission Loss occurred at $\sim 28^{\circ}\text{S}$ and lower loss at $\sim 30^{\circ}\text{S}$ (Figures 9a and c). Generally, there was less Transmission Loss, south of $\sim 29^{\circ}\text{S}$ within the first 50 km. There was also lower loss at the beginning of the spring period, but very little difference between spring and neap tides (Figure 9b).

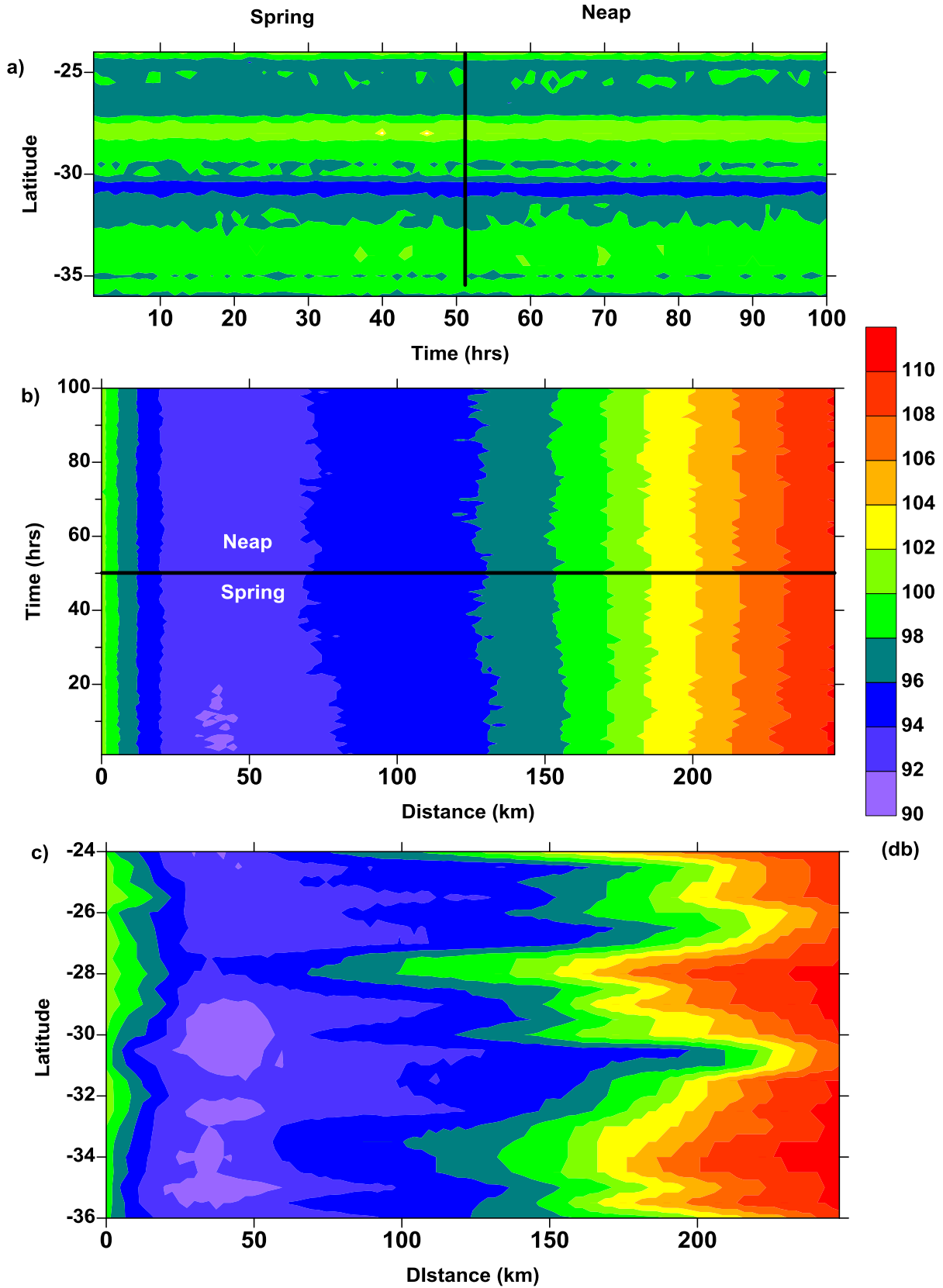


Figure 9. a) Transmission Loss integrated over the entire region with time and latitude for a source depth at 100 m. Transmission Loss integrated over the water column with distance along the ray path with b) time and c) latitude

5. Discussion

The basic pattern of the acoustic ray paths and Transmission Loss were similar for most cases. However, dependencies on latitude, eddies, bottom topography, and source depth did exist. Tidal effects were also evaluated.

5.1 Latitude dependence

The most obvious latitude difference is the three basic regimes and the basic decrease in surface water temperatures with increasing latitude. Horizontal temperature differences are much smaller south of the separation zone than they are across the EAC (Figure 2). The largest temporal fluctuations of the temperature and sound speed occurred in the separation zone (Figure 2). Transmission Loss was smaller south of the EAC region. Factors other than temperature can impact the ray paths. For example, the topography also changes with latitude. Topographic effects are discussed in section 5.2.

5.2 Bottom topography dependence

Besides the temperature fields, the topography changes with latitude both along the coast and in deep water. Along the coast, the primary differences are the width of the continental shelf and the steepness of the continental slope (Figure 1a). In deep water, a chain of seamounts occurs sporadically at different latitudes and distances from the continental slope (Figure 1a). The slope of the continental slope is more gradual in the band from 27°-29°S (Figure 1a). This could have been a factor in the gap in the sound channel formation, since the shape of the continental slope can focus, spread, or block ray paths. However, closer inspection revealed that a seamount ~170 km offshore was driving the rays to the surface forcing them out of a sound channel (not shown). This resulted in the gap in the number of rays in the sound channel for this latitude band (Figure 7b). Not all of the seamounts had this effect and not all of the differences in behaviour with latitude can be attributed to topographic differences, offshore features, such as seamounts, or changes in the slope of the continental slope. Further simulations and analysis are required to pinpoint the specific cause of these effects between topographic, temperature, and latitude differences.

5.3 Eddy dependence

High Transmission Loss occurred in the transect with a large offshore eddy in the EAC regime region (Figure 2a). When the rays reached the location of the well-formed, distinct eddy (90-120 km), their paths altered and Transmission Loss increased (Figure 10). After the eddy, the rays essentially disappear with Transmission Loss at or exceeding 90 dB; whereas before the eddy (~ 90 km), Transmission Loss is <90 dB for nearly the entire water column (Figure 10). Transmission Loss at this latitude, 26°S, is also slightly higher than for its adjacent latitudes (Figure 9c), although significantly less than the loss caused by the seamount at 27°-28°S (see section 5.2).

5.4 Tidal dependence

There was no distinct difference in behaviour between spring and neap tides. However, some of the temporal fluctuations are consistent with the daily and twice daily tidal cycles, particularly the number of rays in the sound channel (Figure 8), the ray depths (Figure 5a and b), and the range of the ray depths (Figure 6a). There was a reduction in the Transmission Loss early in the spring tidal period, but it decreased with time during spring tide (Figure 9b). A more detailed study focussing on the first 50-100 km of the transect where the internal tides are largest or different criteria might reveal stronger tidal impacts. It is more likely that tidal effects on temperature are overshadowed by the effects of eddies and fluctuations in the EAC position and strength.

5.5 Source depth dependence

As seen in a comparison between the upper and lower panels of Figure 4, source depth did impact both

acoustic ray propagation and Transmission Loss. In general, deeper source depths had more rays that did not touch either the surface or the bottom than shallower source depths. With deeper source depths, more rays propagated within the sound channels.

5.6 General observations

Overall, tides had very little influence despite their effect on the sound speed (Figure 3). The EAC and its fronts showed little variability in its impact on the ray paths. The EAC extension region had a series of small eddies along the continental slope. Potentially, these small eddies had similar impacts as the EAC further north, resulting in little variability between the two regions. Thus, with eddies providing similar effects as the EAC, no appreciable latitude dependence was apparent. Also the acoustic rays originated within the EAC or these small eddies, reducing their impact. An earlier study indicated that rays were blocked by eddies, if they originated outside the eddy, but rays originating in an eddy propagated outside of the eddy [3].

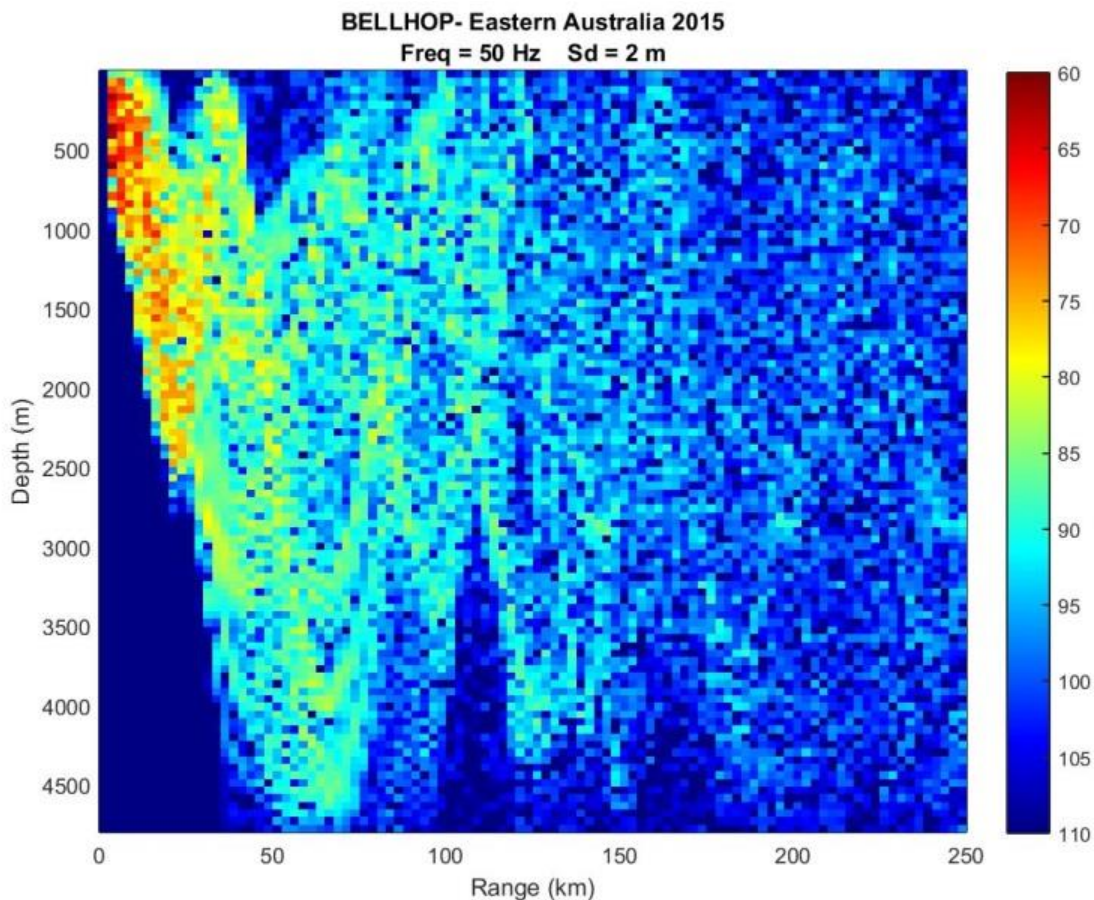


Figure 10. Transmission Loss for the transect at 26°S which had a large offshore eddy centred at ~105 km for a source depth of 2 m and a frequency of 50 Hz.

6. Conclusions

The latitude, topography, eddies, and source depth had the largest impact on the ray paths and Transmission Loss. Tidal impacts were overwhelmed by other features such as eddies. Transmission Loss was the most sensitive parameter to the presence of eddies, seamounts, or other features. Transmission Loss was also lower in the region south of the EAC zone. Topographic features, such as seamounts, were found to impair rays being trapped in sound channels. Eddies increased Transmission Loss and impacted ray paths.

This project is a work in progress and more work needs to be done. Specifically, we would like to improve the criteria on evaluating acoustic propagation and transmission loss, looking into other frequencies, and identifying shadow zones. We note that tidal mixing is strongly latitude dependent

and has significant effects on the temperature field. To distinguish latitude effects from topographic effects, a simulation is required that has the same topographic profiles at all latitudes. Another simulation without any offshore seamounts would remove their effects. Of course, these changes in topography would affect eddy formation and the EAC. We have not done these numerical experiments, since our goal was to look at acoustic propagation in a realistic scenario. We have also not included wind, since we were investigating a climatic hydrography. This neglects upwelling and affects coastal currents. Additionally, the EAC and eddy fields vary seasonally and with climatic factors such as El Niño/La Niña and the Southern Annular mode. These have the potential to impact acoustic propagation. Finally, with climate change, the EAC is pumping more warm water southward, with the result that the waters off Eastern Australia are warming quickly and the EAC is extending further South [11]. This will change the temperature fields in this region and sonar performance in the coming decades.

Acknowledgements

We would like to acknowledge financial support from a UNSW Canberra Defence Related Research Grant.

References

- [1] Frosh, R.A. “Underwater sound: Deep-ocean propagation”, *Science*, **146**, 889-894, (1964).
- [2] Jones, A.D., Zinoviev, A. and Greening, M.V. “A study of the effects on transmission loss of water column features as modelled for an area off the east Australian coast”, *Proceedings of Acoustics 2013*, Victor Harbor, Australia, 17-20 November 2013.
- [3] Clements, J. and Robertson, R. “Acoustic ray propagation in the waters off Eastern Australia using ocean glider data”, *Proceedings of Internoise 2014*, Melbourne Australia, 16-19 November 2014.
- [4] Duda, T.F. “Identifying and meeting new challenges in shallow-water acoustics”, *Proceedings of Acoustics 2013*, Victor Harbor, Australia, 17-20 November 2013.
- [5] Cooper, J. *An investigation into the effects of internal tides on acoustic propagation in the Indonesian seas*, Honours Thesis, University of New South Wales Canberra, 2011.
- [6] Robertson R. and Hartlipp, P.S. “Tidal effects on acoustic propagation off Eastern Australia”, *Proceedings of Internoise 2014*, Melbourne Australia, 16-19 November 2014.
- [7] Rodrigues, O.C. *General description of the BELLHOP ray tracing program*, Universidade do Algarve, 2008. <http://oalib.hlsresearch.com/Rays/GeneralDescription.pdf>
- [8] Porter, M.B. *The BELLHOP Manual and User’s Guide* <http://oalib.hlsresearch.com/Rays/HLS-2010-1.pdf>, 2011
- [9] Hartlipp, P.S. and Robertson, R. “Internal tides off the eastern Australian coast: A comparison to observations”, *Journal of Geophysical Research: Oceans*, in preparation, 2015.
- [10] Fofonoff, N.P. and Millard, R.C. Jr. Algorithms for computation of fundamental properties of seawater, *UNESCO Technical Paper in Marine Science*, **44**, Division of Marine Sciences, 1983.
- [11] Robertson, R., Doblin, M., Ingleton, T., Suthers, I., Roughan, M. et al. “The East Australian Current and its interaction with coastal environments”, *NSW-IMOS Node Science and Implementation Plan 2015-2025*, 2014
http://imos.org.au/fileadmin/user_upload/shared/IMOS%20General/documents/IMOS/Plans/Reports/Science_Implementation_Plans/NSW-IMOS_Node_Plan_2015-25_Final_25-9-14.pdf,